

This discussion paper is/has been under review for the journal Atmospheric Chemistry and Physics (ACP). Please refer to the corresponding final paper in ACP if available.

## Ice nuclei properties at the Jungfraujoch within a Saharan Dust Event

C. Chou et al.

# Ice nuclei properties within a Saharan Dust Event at the Jungfraujoch

C. Chou<sup>1</sup>, O. Stetzer<sup>1</sup>, E. Weingartner<sup>2</sup>, Z. Jurányi<sup>2</sup>, Z. A. Kanji<sup>1</sup>, and U. Lohmann<sup>1</sup>

<sup>1</sup>ETH Zurich, Institute for Atmospheric and Climate Science, Switzerland

<sup>2</sup>Laboratory of Atmospheric Chemistry, Paul Scherrer Institut, Villigen PSI, Switzerland

Received: 7 September 2010 – Accepted: 23 September 2010 – Published: 12 October 2010

Correspondence to: C. Chou (cedric.chou@env.ethz.ch)

Published by Copernicus Publications on behalf of the European Geosciences Union.

Title Page

Abstract

Introduction

Conclusions

References

Tables

Figures

⏪

⏩

◀

▶

Back

Close

Full Screen / Esc

Printer-friendly Version

Interactive Discussion

## Abstract

The new portable ice nucleation chamber (PINC) developed by the Institute for Atmospheric and Climate Sciences of ETH Zurich was operated during two campaigns PINC II and III at the high alpine research station Jungfraujoch situated at 3580 m a.s.l., in March and June 2009, respectively. During this time of the year, a high probability of Saharan Dust Events (SDE) at the Jungfraujoch has been observed. We used an impactor with a cutoff size of 1  $\mu\text{m}$  aerodynamic diameter and operated the system at  $-31^\circ\text{C}$  and relative humidities of 127% and 91% with respect to ice and water, respectively in order to investigate the contribution of deposition freezing to mixed-phase clouds and also to look at the number concentration of ice nuclei (IN) during a SDE. The average IN concentration during PINC II was 8 particles per liter whereas during PINC III, the average number concentration was higher up to 14 particles per liter. Two SDEs were detected on 15 and 16 June 2009. Our measurements show that the SDEs had IN number concentration up to several hundreds per liter. We found the best correlation between the number concentration of the larger particle fraction measured by an optical particle counter and the IN number concentration during a Saharan Dust Event. This correlation factor is higher for particles larger than 0.5  $\mu\text{m}$  meaning that a higher concentration of larger particles induced higher IN number concentration. No correlation could be found between the black carbon mass concentration and the variations in IN number concentration.

## 1 Introduction

Atmospheric aerosols contribute to the largest uncertainty in the global radiative forcing since pre-industrial times (Forster et al., 2007). On one hand aerosols have the ability to scatter and/or absorb the incoming solar and terrestrial radiation (aerosol direct effect), e.g., Haywood and Boucher (2000). On the other hand, aerosols play a major role in the formation of clouds, and govern their lifetime as well as their microphysical

## Ice nuclei properties at the Jungfraujoch within a Saharan Dust Event

C. Chou et al.

Title Page

Abstract

Introduction

Conclusions

References

Tables

Figures

⏪

⏩

◀

▶

Back

Close

Full Screen / Esc

Printer-friendly Version

Interactive Discussion



properties. This has an influence on precipitation and also on the radiative budget (aerosol indirect effect), e.g. Lohmann and Feichter (2005). The ice phase in mixed-phase clouds is of crucial importance, as 70% of the total precipitation forms via the ice phase (Lau and Wu, 2003). Ice crystals in the atmosphere form via two pathways: homogeneous and heterogeneous freezing. Homogeneous nucleation is significant at temperatures below  $-38^{\circ}\text{C}$ . At higher temperatures the formation of ice in clouds is triggered by heterogeneous freezing which is divided into four sub-processes: Immersion, condensation, contact and deposition nucleation (Vali, 1985). Laboratory experiments have shown that mineral dust is a good ice nucleus (IN) in both immersion and deposition freezing mode (Mason and Maybank, 1958; Isono et al., 1959; Roberts and Hallett, 1968; Schaller and Fukuta, 1979; Mangold et al., 2005; Möhler et al., 2006) and usually initiates nucleation at rather high temperatures and low relative humidities. This statement is supported by field studies (DeMott et al., 2003b; Richardson et al., 2007; Klein et al., 2010) where high concentrations of mineral dust led to a significant increase in the ice crystal number concentration. More recent studies by Möhler et al. (2008) showed that bioaerosols and especially some specific bacteria like *Pseudomonas Syringae* initiate ice formation at warmer temperatures than mineral dust. Pratt et al. (2009) found that one third of the ice particle residues in one cloud collected by a Counterflow Virtual Impactor (CVI) at high altitude over Wyoming contained biological markers. Soot and particles containing black carbon (BC) are also known to act as IN, but require much lower temperatures and higher relative humidities for activation as compared to bioaerosols and mineral dust (DeMott et al., 1999; Dymarska et al., 2006). Dymarska et al. (2006) showed that in order to trigger deposition freezing, soot require temperatures lower than  $-30^{\circ}\text{C}$  and relative humidity with respect to water close to saturation. Nevertheless Cozic et al. (2008a) found that ice residuals in mixed-phase clouds collected at the high alpine research station Jungfraujoch (JFJ) in Switzerland have a BC mass enrichment of 27%. As the temperature at the station is never lower than  $-30^{\circ}\text{C}$ , these measurements raise some questions: do BC particles form ice mainly via immersion or/and contact freezing at the Jungfraujoch? Do these

## Ice nuclei properties at the Jungfraujoch within a Saharan Dust Event

C. Chou et al.

[Title Page](#)[Abstract](#)[Introduction](#)[Conclusions](#)[References](#)[Tables](#)[Figures](#)[Back](#)[Close](#)[Full Screen / Esc](#)[Printer-friendly Version](#)[Interactive Discussion](#)

BC particles have different properties than those produced in laboratory and have enhanced IN properties in the deposition mode? The ice nucleation properties of BC are still unclear as a recent study conducted by Kamphus et al. (2010) at the JFJ during the Cloud and Aerosol Characterization Experiment 6 (CLACE-6) showed no enrichment of BC in the particles analyzed.

So far, very few studies with chambers have been performed in-situ in the free or upper troposphere, where conditions are favorable for the formation of mixed-phase and ice clouds. Those studies are summarized in Möhler et al. (2007) and showed that the IN number concentration could vary from 0.01 to 50 particles per liter for different regions, seasons and altitude. In order to have additional data at different locations in the world and information on IN properties of atmospherically relevant aerosols, two measurement campaigns (PINC II and PINC III) were conducted at the JFJ. A previous study has been conducted at the JFJ in order to characterize ice crystals sampled in mixed-phase clouds (Mertes et al., 2007). They found during CLACE-3 an average concentration of several hundreds ice residuals per liter in one cloud on 24 March 2004 using an ice-CVI. PINC II and III were also motivated by the high probability of Saharan Dust Events (SDE) between March and June (Collaud Coen et al., 2004). This paper discusses results of IN number concentration and its variation with respect to a SDE at JFJ. Correlation between BC and IN concentrations are also discussed.

## 2 Experimental setup

### 2.1 Ice nuclei measurements

#### 2.1.1 The portable ice nucleation chamber

The Portable Ice Nucleation Chamber (PINC) has recently been developed in order to measure IN concentrations during airborne and field campaigns. It is the portable version of the Zurich Ice Nucleation Chamber (ZINC) (Stetzer et al., 2008) and its principle

## Ice nuclei properties at the Jungfrauoch within a Saharan Dust Event

C. Chou et al.

Title Page

Abstract

Introduction

Conclusions

References

Tables

Figures

⏪

⏩

◀

▶

Back

Close

Full Screen / Esc

Printer-friendly Version

Interactive Discussion



follows the Continuous Flow Diffusion Chamber (CFDC) of the University of Colorado (Rogers, 1988). There are two main differences between ZINC and PINC, the cooling system and the size. Briefly, it consists of two flat parallel plate walls which can be cooled independently of each other to temperatures as low as  $-47^{\circ}\text{C}$  for the warm side and  $-55^{\circ}\text{C}$  for the cold side. Before a measurement, the chamber is flooded with water for a short period in order to produce a thin ice layer on the walls which then is maintaining a constant relative humidity of ice saturation on the wall surface. By applying a temperature difference between both walls, diffusion of water vapor leads to a supersaturation within the chamber which depends on the position between the walls and the temperature gradient. A continuous flow of sample air, typically 1 lpm (liter per minute) – layered between two particle-free sheath flows, typically 4.5 lpm each – is drawn through the chamber to expose the sample to a defined supersaturation and temperature for a duration of about 8 s. It is important to mention that PINC can only measure in the deposition and condensation freezing modes and to some extent in the homogeneous freezing mode. The major difference between our established lab-instrument ZINC and the new PINC instrument is the portable and lightweight cooling system and the reduced chamber length (95 cm for PINC versus 180 cm for ZINC) so that the instrument fits into existing research aircraft. The PINC cooling system consists of two independent compressor-based refrigeration systems where the evaporation tubes made out of copper are firmly inserted into drilled channels on the outer sides of the chamber walls. Because a measurement requires a temperature gradient between the walls, the two systems are not identical. Hence, the cooling system for the warmer wall consists of two parallel compressors (BD120, Danfoss) while the colder wall system has in total 5 compressors of the same kind, but connected in a 4+1 manner, meaning 4 parallel units combined with one further in series to obtain a higher compression to reach lower temperatures. More details are shown in Fig. 1. The BD120 compressors were chosen because they are specially made for mobile applications. They run on 24 Volts DC and their cooling power can be regulated over a wide range with pulse-width-modulation (PWM) drivers. They also tolerate tilting of the instrument

## Ice nuclei properties at the Jungfraujoch within a Saharan Dust Event

C. Chou et al.

[Title Page](#)[Abstract](#)[Introduction](#)[Conclusions](#)[References](#)[Tables](#)[Figures](#)[Back](#)[Close](#)[Full Screen / Esc](#)[Printer-friendly Version](#)[Interactive Discussion](#)

## Ice nuclei properties at the Jungfraujoch within a Saharan Dust Event

C. Chou et al.

Title Page

Abstract

Introduction

Conclusions

References

Tables

Figures

⏪

⏩

◀

▶

Back

Close

Full Screen / Esc

Printer-friendly Version

Interactive Discussion



while in operation and are therefore well suited for airborne instruments. In laboratory tests, we reached sampling conditions of  $-45^{\circ}\text{C}$  with a relative humidity with respect to ice ( $\text{RH}_i$ ) of 158% and a relative humidity with respect to water ( $\text{RH}_w$ ) of 100%. At these conditions, the wall temperatures are at 222 K and 240 K for the cold and the warm wall, respectively. In parallel to the evaporation tubes, several heating pads are attached to each wall which help when positive temperature changes are needed for one wall and to compensate for possible temperature inhomogeneities within a wall.

The instrument has a short isothermal evaporation section attached at the bottom of the main chamber, which is cooled by the warm wall cooling system and thus is maintained at the warm wall temperature, allowing the section to be saturated with respect to ice but subsaturated with respect to water. Thus, the section allows evaporation of droplets which may form at/or above water saturation so that they are not falsely counted as ice crystals by the optical particle counter (OPC) (Climet, OI 3100). The residence time of a particle in this section is 2.4 s and depending on the evaporation section temperature, droplets will evaporate slower or faster. Figure 2 shows the maximum  $\text{RH}_w$  we can reach before water droplets formed inside the chamber can survive and be falsely counted as ice crystals by the OPC. The data acquisition system of PINC is similar to the one of ZINC (Stetzer et al., 2008) but uses the more up-to-date CRIO architecture (National Instruments). This consist of a real-time computer running a specialized version of the Labview programming language. It also has a FPGA (field programmable gate array) chip to implement certain parts of the code which directly reads from input and writes to output modules in hardware. Code on the FPGA is very fast and efficient. We take advantage of this by using simple high-current digital output modules to regulate the power of heatings and compressors with software PWM drivers which are running inside the FPGA chip.

### 2.1.2 Large particles and wet particles issues

The current setup of PINC uses an OPC to detect ice crystals by size. A particle is classified as ice crystal by the OPC when its optical diameter is larger than  $3\ \mu\text{m}$ .

Since PINC has been designed for field and in-situ measurements, the presence of large particles as well as water droplets cannot be excluded.

In order to remove the large particle fraction, we used the impactor built for the Differential Mobility Analyser (DMA) from TSI with an orifice of 0.071 cm. Several laboratory tests with an Aerodynamic Particle Sizer (APS) (TSI, model 3321) and a Scanning Mobility Particle Sizer (SMPS) (TSI, model 3080) sampling ambient air have been performed and Fig. 3 shows the impactor efficiency for different aerodynamic sizes. The cutoff  $d_{50}$  is at 0.91  $\mu\text{m}$ , aerodynamic diameter. Table 1 shows the conversion between aerodynamic and optical diameter following Baron and Willeke (2001) (see Eq. 1) as we need both diameters:

$$d_a = d_p \cdot \left( \frac{\rho_p}{\rho_0} \right)^{\frac{1}{2}}, \quad (1)$$

with  $d_a$  the aerodynamic diameter,  $d_p$  the diameter of a spherical particle,  $\rho_p$  the particles density and  $\rho_0$  the standard density of a spherical particle, typically 1  $\text{g}/\text{cm}^3$ . Cozic et al. (2008b) showed that the submicron particle average density at the JFJ was 1.5  $\text{g}/\text{cm}^3$ , which is the value we use for the conversion in Table 1.

The main objective of this study is to focus on deposition nucleation mode, so it is crucial that the particles sampled are dry. In order to do so, we use a molecular sieve diffusion drier mounted in front of the system. The relative humidity measured at the exit of the diffusion drier is 1% (with a sensor accuracy of  $\pm 2\%$ ), which is sufficient to remove the moisture from the particles. The particle gravitational loss is 2% for the larger size sampled i.e. 1  $\mu\text{m}$ , and the diffusion loss for the smallest particles we expect to be IN (100 nm) is below 1%.

### 2.1.3 Validation experiments using ammonium sulphate aerosol

The sample temperature and relative humidities are calculated from the measured temperatures of the main chamber walls. In order to validate the accuracy of the calculated temperature and relative humidities at the sample position inside the chamber,

## Ice nuclei properties at the Jungfraujoch within a Saharan Dust Event

C. Chou et al.

Title Page

Abstract

Introduction

Conclusions

References

Tables

Figures

⏪

⏩

◀

▶

Back

Close

Full Screen / Esc

Printer-friendly Version

Interactive Discussion



the deliquescence and freezing points of ammonium sulphate (AS) aerosols were investigated at different thermodynamic conditions, because they are well known from the literature. Figure 4 shows the setup of the experiment. Ammonium sulphate particles were produced from a 3% (by weight) AS solution which was then atomized. The droplets went through a molecular sieves diffusion drier to crystallize the droplets. The particles were then size selected with the DMA attached to the SMPS before entering PINC. Validation experiments were performed with 200 nm particles at two temperatures,  $-30^{\circ}\text{C}$  and  $-40^{\circ}\text{C}$ . The experiments at  $-30^{\circ}\text{C}$  showed deliquescence of the particles at 84%  $\text{RH}_w$  at the sample position which is in good agreement by  $\pm 2\%$  with the values obtained by Braban et al. (2001); Kanji and Abbatt (2006). In order to see at which conditions AS could freeze homogeneously, we operate the chamber at  $-40^{\circ}\text{C}$  which is below the temperature of homogeneous freezing, and set a  $\text{RH}_w$  above the deliquescence point of AS. We found that AS froze homogeneously at relative humidities of 145% and 97% with respect to ice and water, respectively. These values also agree by  $\pm 2\%$  with the theoretical values calculated by Koop et al. (2000) based on the water activity for a 200 nm diameter aerosol particle.

#### 2.1.4 Operating conditions during PINC II and III

IN number concentration measurements took place during PINC II (from 24 February–10 March 2009) and PINC III (from 3–17 June 2009) at the JFJ research station situated at an altitude 3580 m a.s.l. ( $46^{\circ}33' \text{N}$  by  $7^{\circ}59' \text{E}$ ). The JFJ is mostly in free tropospheric conditions and is a Global Atmosphere Watch (GAW) station where aerosols and gases have been measured for several years. Further description of the measurement site are given in Baltensperger et al. (1997).

Kanji and Abbatt (2006) showed that at  $-30^{\circ}\text{C}$ , the nucleation onset of Saharan dust was below a  $\text{RH}_i$  of 110% in the deposition mode. Thus in order to activate any possible Saharan dust present at the JFJ, the operating conditions of PINC during this campaign at the sample position were set to  $-31^{\circ}\text{C}$  (which is a relevant temperature for mixed-phase clouds), with a  $\text{RH}_i$  of 127% ( $\text{RH}_w=91\%$ ). Every measurement point reported in

### Ice nuclei properties at the Jungfraujoch within a Saharan Dust Event

C. Chou et al.

Title Page

Abstract

Introduction

Conclusions

References

Tables

Figures

⏪

⏩

◀

▶

Back

Close

Full Screen / Esc

Printer-friendly Version

Interactive Discussion



Figs. 5, 8, 11 and 12 is a 15 min average, with a five second interval between each IN count. Due to background signal coming from the chamber, a blank measurement (no aerosol injected) at the beginning and at the end of a measurement is taken in order to obtain an average background value that can be subtracted from the 15 min average measurement. This background signal is coming from ice peaks that have grown on the walls of the chamber, and is typically less than 3 particles per liter. We usually re-ice the chamber after 2 h of ambient measurements, when the background signal exceeds 5 particles per liter.

## 2.2 Black carbon measurements

Downstream of the inlet, a Multi-Angle Absorption Photometer (MAAP, Thermo ESM, Andersen) operated at a nominal wavelength of  $\lambda=630$  nm (Petzold and Schönlinner, 2004) was used to measure the light absorption coefficient from which the BC mass concentration was derived using a mass absorption efficiency of  $6.6 \text{ m}^2/\text{g}$ .

## 2.3 Detection of Saharan Dust Events

The dry particle scattering coefficient  $\sigma_{\text{sp}}$  was measured by an integrated nephelometer (IN, TSI 3563) simultaneously at three different wavelengths ( $\lambda=450, 550$  and  $700$  nm). The data are collected with a five minutes resolution and an hourly average was calculated from these data. The absorption coefficient  $\sigma_{\text{ap}}$  was measured by an aethalometer (AE-31, Magee Scientific) at seven wavelengths ( $\lambda=370, 470, 520, 590, 660, 880$  and  $950$  nm). The calculation of  $\sigma_{\text{ap}}$  was done following Weingartner et al. (2003).

The scattering and absorption coefficients are used to derive the single scattering albedo (SSA) exponent  $\alpha$ , which describes the wavelength dependence of the SSA:

$$\text{SSA} = b_{\text{SSA}} \times \lambda^{-\alpha_{\text{SSA}}}, \quad (2)$$

A dust event is notified only if the SSA exponent is negative for more than 4 h consecutively. More details can be found in Collaud Coen et al. (2004).

# Ice nuclei properties at the Jungfraujoch within a Saharan Dust Event

C. Chou et al.

[Title Page](#)[Abstract](#)[Introduction](#)[Conclusions](#)[References](#)[Tables](#)[Figures](#)[⏪](#)[⏩](#)[◀](#)[▶](#)[Back](#)[Close](#)[Full Screen / Esc](#)[Printer-friendly Version](#)[Interactive Discussion](#)

These instruments were complemented by an optical particle counter (OPC, Grimm Dust monitor 1.108) measuring the dry particle size distribution in the diameter range of 0.3 to 20  $\mu\text{m}$  behind the total aerosol inlet. The factory calibration of the OPC was done with LATEX spheres. Schwikowski et al. (1995) found that there is an increase in the coarse fraction of the aerosol size distribution during a SDE, suggesting that an increase in the supermicron mode detected by the OPC is also a good indicator of dust load at the JFJ.

In order to predict a SDE we used the BSC-DREAM dust model forecast (Nickovic et al., 2001; Pérez et al., 2006a,b) from the Barcelona Supercomputing Center (BSC). Distribution of dust load around the Mediterranean region can be forecasted 72 h in advance, and wind profiles can also be observed. In complement, we used that tool in combination with the Lagranto model (Wernli and Davies, 1997) to calculate backtrajectories arriving at the JFJ during the days of interest. This allow us to investigate the origin of air masses and to interpretate our data.

## 3 Results and discussion

### 3.1 Ice nuclei number concentration

#### 3.1.1 Non-SDE days

Due to some instrumentation problems, some days during both campaigns are not reported in the figures. IN number concentration in the deposition freezing mode from 1 to 10 March are reported in Fig. 5a. The IN number concentration for the first 8 days is below 10 particles per liter, however there is an increase on 9 and 10 March. The IN number concentration during these two days reached 20 particles per liter. By investigating the SSA exponent, we can see that on 9 March, the exponent was below zero for short periods of time, suggesting that there was a possibility of mineral dust being present. On 10 March, the SSA exponent was positive most of the sampling time. In

## Ice nuclei properties at the Jungfraujoch within a Saharan Dust Event

C. Chou et al.

Title Page

Abstract

Introduction

Conclusions

References

Tables

Figures

⏪

⏩

◀

▶

Back

Close

Full Screen / Esc

Printer-friendly Version

Interactive Discussion



order to trace a possible presence of dust, backward trajectories have been calculated for these two days to see if a SDE was passing through the research station. Figure 7 shows the 4-day backtrajectories and Fig. 6 shows the dust load over Northern Africa and Europe. Both backward trajectories show no evidence of dust arriving at JFJ, meaning that the higher IN number concentration on these two days must have a different source. We speculate that this increase could be connected to higher biological activity coming from plants (mainly bacteria regarding their size and our cutoff size), but due to the lack of bio-detection instruments, this assumption can not be verified. The average IN number concentration of the measurement period of PINC II is 8 particles per liter. In comparison, Mertes et al. (2007) found a number of ice residuals two orders of magnitude higher than our results. This can be explained by the fact that we are investigating only one freezing mode, neglecting immersion, condensation and contact freezing. Moreover, we have restricted our size range of particles sampled up to 1  $\mu\text{m}$  aerodynamic diameter. Finally, the ice residuals sampled might have had another origin and were not formed recently before it was collected by the ice-CVI.

In Fig. 8a, the IN number concentration from 10 to 16 June is shown. The average ambient IN number concentration (not influenced by SDEs) is around 14 particles per liter which is twice as high as at the beginning of March. Klein et al. (2010) has recently found a IN number concentration of about 40 IN per liter at the Taunus Observatory at a temperature of  $-18^{\circ}\text{C}$ . It is important to mention that in their study, the particle size range sampled is from 0.2 to 12  $\mu\text{m}$  whereas we sampled particles with an upper size limit of 1  $\mu\text{m}$  aerodynamic diameter. Furthermore they might have a constant influence of the Planetary Boundary Layer (PBL), which contributes to a higher number of particles, meaning more potential IN. As another comparison, Richardson et al. (2007) using a CFDC found IN number concentration varying from 1 to 10 IN per liter during Spring at the Storm Peak Laboratory (SPL) situated in the Rocky Mountains of Northwestern Colorado (USA). The SPL is located at 3210 m above mean sea level (MSL) and is comparable to the altitude of the Jungfraujoch. The average IN number concentration found during our campaigns are in good agreement with their results

## Ice nuclei properties at the Jungfraujoch within a Saharan Dust Event

C. Chou et al.

[Title Page](#)[Abstract](#)[Introduction](#)[Conclusions](#)[References](#)[Tables](#)[Figures](#)[Back](#)[Close](#)[Full Screen / Esc](#)[Printer-friendly Version](#)[Interactive Discussion](#)

at the same thermodynamic conditions. Higher concentrations (>25 IN/liter) could be observed on four different days, 11, 14, 15 and 16 June. This is discussed in the following sections.

### 3.1.2 During a SDE

Two SDE occurred on 15 and 16 June (see Fig. 8) according to the methodology discussed in Sect. 2.3 and used by Collaud Coen et al. (2004) to assess the presence of SDE. The IN number concentration increased by 10 to 20 times compared to typical IN concentrations. This result is in good agreement with the results from DeMott et al. (2003b) who found a significant increase in IN number concentration of 20 to 100 times when they sampled within transported African dust layers over Florida. Note that the operating temperature during PINC III was 5 °C higher than that of the CFDC during the DeMott et al. (2003b) study. This high increase in IN number concentration is in very good agreement with the recent study by Klein et al. (2010) who found a concentration of IN 10 times higher than a typical day during a Saharan dust episode at the Taunus Observatory in Germany. On 16 June the IN number concentration is slightly higher than on a typical measurement day due to the SDE contribution, but is less intense than the one on 15 June. This is supported by Fig. 8d which shows the time series of the aerosol particle concentration in the accumulation mode. The particle number concentration on 16 June is only half of that measured on 15 June meaning that other parameters like the chemical composition of mineral dust or its size might play a role as the IN number concentration is about 10 times higher on 15 June than on 16 June. We investigated the dust load and backward trajectories shown in Figs. 9 and 10, respectively, to trace the sources of the mineral dust we sampled. Figure 9 shows that on 15 June the air mass was coming from North Africa, where the dust concentration was high (around 0.75 g/m<sup>2</sup>). On the other hand, on 16 June, the air mass came from the North Atlantic Ocean where a low dust load was present (<0.3 g/m<sup>2</sup>). This may explain the difference in the concentration of ice crystals measured on these two days.

## Ice nuclei properties at the Jungfraujoch within a Saharan Dust Event

C. Chou et al.

Title Page

Abstract

Introduction

Conclusions

References

Tables

Figures

⏪

⏩

◀

▶

Back

Close

Full Screen / Esc

Printer-friendly Version

Interactive Discussion



### 3.1.3 High IN number concentration during non SDE

Two SDE were clearly detected via optical means but the intensity was totally different. On 11 June (afternoon) and 14 June, higher concentration as compared to 16 June were observed, but as shown in Fig. 8, the SSA exponent was not negative. Figures 9 and 10 show that air masses on 14 June were coming from North Africa and contain high dust loads which would explain the increase in IN number concentration on that day. In comparison with 15 June, the IN concentration is more irregular on 14 June. We observed a very high concentration in the morning followed by a decrease at noon. Then in the beginning of the afternoon, high IN concentration could be observed again followed by a steep drop in the evening. These variations in concentration at noon can be explained by the fact that during summer, the JFJ can be influenced by the PBL, therefore increasing the aerosol number concentration in the accumulation mode for a short period if the PBL is oscillating around the altitude of the research station. Note that investigating the number concentration of the accumulation mode is a good indicator of the PBL influence (Nyeki et al., 1998). This is supported by data shown in Fig. 8d, where we observe oscillation in the accumulation mode concentration with a maximum in the morning, followed by a steep decrease at noon. Then, an increase in the early afternoon is followed by a decrease towards the evening. These oscillations in dust concentrations can also explain why the SDE on 14 June was not detected by optical means. As described in Sect. 2.3, a SDE is considered to occur only if the SSA exponent is negative for at least four hours consecutively. The contribution of the dust load was probably not high enough to influence  $\sigma_{sp}$ . On 11 June, the air masses arriving at the JFJ did not contain any dust according to Figs. 9 and 10, but a sudden increase could be observed at around 05:00 p.m., for a short time. Figure 8c shows that at this time, the SSA exponent started to be  $<0$  which suggest that it may have been a dust contribution that had been transported across the North Atlantic Ocean to the JFJ research station.

## Ice nuclei properties at the Jungfraujoch within a Saharan Dust Event

C. Chou et al.

Title Page

Abstract

Introduction

Conclusions

References

Tables

Figures



Back

Close

Full Screen / Esc

Printer-friendly Version

Interactive Discussion



### 3.2 Correlations of IN with mineral dust

Previous studies (Archuleta et al., 2005; Welte et al., 2009; Kanji and Abbatt, 2009) showed that the size of mineral dust plays an important role in the ice nucleation efficiency of the particles, and that the larger, the more efficient the particles are. This is confirmed by Mertes et al. (2007); Kamphus et al. (2010) who found a larger number concentration of larger particles in the ice residuals sampled during CLACE-3 and 6, respectively. As mentioned in Sect. 2.3, Schwikowski et al. (1995) showed that the concentration of larger particles is higher during a dust event than for a non SDE event. We investigate a possible correlation between the IN number concentration and the increase in number of larger particles. We used data from the OPC (Grimm Dust monitor 1.108) connected to the total aerosol inlet that counts particles in a size range from 0.3  $\mu\text{m}$  to 20  $\mu\text{m}$ . Due to the use of an impactor connected at the entrance of PINC, we only investigate particle sizes up to 0.8  $\mu\text{m}$ . The OPC data are also averaged in order to match the time resolution of the IN measurements. Figure 11 shows the IN number concentration as a function of each size class for PINC II and III. Particles of  $0.3 < \text{diameter}(D) < 0.5 \mu\text{m}$  show a correlation coefficient  $R^2$  of 0.69 (see Table 2) whereas particles of  $0.5 < D < 0.8 \mu\text{m}$  show a better correlation ( $R^2=0.88$ ) with the IN number concentration. This correlation suggests that the higher concentration of particles larger than 0.5  $\mu\text{m}$ , the higher IN number concentration we detect. This method is complementary to the one used by Collaud Coen et al. (2004), as it allows the detection of dust for a short period as for example the observation on 14 June.

### 3.3 Correlations of IN with BC

One of our motivations was to investigate if the formation of ice crystals could have been influenced by the presence of BC. It is important to note that IN are counted as number concentration whereas the BC concentration is expressed in mass concentrations. We have integrated the BC mass concentration (derived from the MAAP) over 15 min to match the time of our IN measurements. During a SDE the absorption

## Ice nuclei properties at the Jungfraujoeh within a Saharan Dust Event

C. Chou et al.

Title Page

Abstract

Introduction

Conclusions

References

Tables

Figures

⏪

⏩

◀

▶

Back

Close

Full Screen / Esc

Printer-friendly Version

Interactive Discussion



coefficient increases due to absorbant compounds found in mineral dust. In order to avoid biases due to SDE, and also to assess which other types of particles might act as IN during a non SDE day, we have only investigated the BC dependency on non SDE days as shown in Fig. 12. The correlation coefficient  $R^2$  between the BC concentration and the IN number concentration is 0.12. It is thus not possible to conclude that BC has an impact on the variation of the IN number concentration, although Cozic et al. (2008a) found an enrichment in BC in the ice residuals measured during three CLACE campaigns. In addition, the MAAP derives a BC concentration from a calculated absorption coefficient, meaning that some absorbant compounds could falsely be classified as BC, and this is especially the case in presence of high concentrations of mineral dust (Collaud Coen et al., 2004). This weak correlation found is however in good agreement with the recent study of Kamphus et al. (2010) which found no BC enrichment in the ice residuals during CLACE 6.

## 4 Conclusions

This paper discussed in-situ measurements of IN number concentration and their properties during Saharan Dust Events at the high alpine research station Jungfraujoch (JFJ) at ambient thermodynamic conditions. We showed that the IN number concentration can increase by one order of magnitude during a SDE, but can also increase by just a factor of 2, suggesting that SDE have different intensities but also that their properties might play an important role in the ice nucleation efficiency of the particles. Future work at the JFJ will require instrumentation that can measure the chemical composition as a function of the size of the particles as was done in the DeMott et al. (2003a) study. We also showed that we have a better correlation between the IN number concentration and the larger aerosol particles (counted by the optical particle counter).

Investigation of the BC dependence of the IN concentration has been performed as well, and the results showed that there is no correlation between BC mass

### Ice nuclei properties at the Jungfraujoch within a Saharan Dust Event

C. Chou et al.

Title Page

Abstract

Introduction

Conclusions

References

Tables

Figures



Back

Close

Full Screen / Esc

Printer-friendly Version

Interactive Discussion



concentration and IN number concentration. However this is not conclusive and single particle analysis would be required to see if the ice crystals formed in PINC contain BC. Another important fact is that we worked at conditions where only deposition freezing could take place, meaning that both condensation and immersion freezing onto particles sampled are not investigated. Furthermore, particles larger than 1  $\mu\text{m}$  were not entering the chamber, thus reducing the IN number concentration investigated. BC particles could trigger nucleation via immersion or contact freezing which this study did not investigate. Investigation of immersion freezing with the new chamber IMCA developed at our institute (Lüönd et al., 2010) in combination with a Soot Photometer (SP2) could help to investigate the possible role of BC in future campaigns.

*Acknowledgements.* We would like first to thank Hannes Wydler for all the technical work done on PINC. We would like to thank A. Welti, A. Ćirišan, V. Sant and F. Lüönd for software support. We acknowledge the costudians of the High Alpine Research Station, the Fischer and Seiler. We are also grateful to L. Wilson for the organisation of the campaigns, and Prof. Dr. Flueckiger for allowing us to perform measurements. We acknowledge the financial support of the Global Atmospheric Watch (GAW) program. Finally we would like to thank the Barcelona Supercomputing Center operator for providing the data and images from the BSC-DREAM8b (Dust REgional Atmospheric Model) model, operated by the Barcelona Supercomputing Center (<http://www.bsc.es/projects/earthscience/DREAM/>).

## References

- Archuleta, C. M., DeMott, P. J., and Kreidenweis, S. M.: Ice nucleation by surrogates for atmospheric mineral dust and mineral dust/sulfate particles at cirrus temperatures, *Atmos. Chem. Phys.*, 5, 2617–2634, doi:10.5194/acp-5-2617-2005, 2005. 23718
- Baltensperger, U., Gäggeler, H., Jost, D., Lugauer, M., Schwikowski, M., Weingartner, E., and Seibert, P.: Aerosol climatology at the high-alpine site Jungfraujoch, Switzerland, *J. Geophys. Res.-Atmos.*, 102, 19707–19715, doi: 10.1029/97JD00928 1997. 23712
- Baron, P. and Willeke, K.: *Aerosol Measurement: Principles, Techniques, and Applications*, Wiley-Interscience, New York, 2001. 23711, 23725

## Ice nuclei properties at the Jungfraujoch within a Saharan Dust Event

C. Chou et al.

Title Page

Abstract

Introduction

Conclusions

References

Tables

Figures

⏪

⏩

◀

▶

Back

Close

Full Screen / Esc

Printer-friendly Version

Interactive Discussion



## Ice nuclei properties at the Jungfrauoch within a Saharan Dust Event

C. Chou et al.

[Title Page](#)
[Abstract](#)
[Introduction](#)
[Conclusions](#)
[References](#)
[Tables](#)
[Figures](#)




[Back](#)
[Close](#)
[Full Screen / Esc](#)
[Printer-friendly Version](#)
[Interactive Discussion](#)


- Braban, C., Abbatt, J., and Cziczo, D.: Deliquescence of ammonium sulfate particles at sub-eutectic temperatures, *Geophys. Res. Lett.*, 28, 3879–3882, doi:10.1029/2001GL013175, 2001. 23712
- Collaud Coen, M., Weingartner, E., Schaub, D., Hueglin, C., Corrigan, C., Henning, S., Schwikowski, M., and Baltensperger, U.: Saharan Dust Events at the Jungfrauoch: detection by wavelength dependence of the single scattering albedo and first climatology analysis, *Atmos. Chem. Phys.*, 4, 2465–2480, doi:10.5194/acp-4-2465-2004, 2004. 23708, 23713, 23716, 23718, 23719
- Cozic, J., Mertes, S., Verheggen, B., Cziczo, D., Gallavardin, S., Walter, S., Baltensperger, U., and Weingartner, E.: Black carbon enrichment in atmospheric ice particle residuals observed in lower tropospheric mixed phase clouds, *J. Geophys. Res.*, 113, D15209, doi:10.1029/2007JD009266, 2008a. 23707, 23719
- Cozic, J., Verheggen, B., Weingartner, E., Crosier, J., Bower, K. N., Flynn, M., Coe, H., Henning, S., Steinbacher, M., Henne, S., Collaud Coen, M., Petzold, A., and Baltensperger, U.: Chemical composition of free tropospheric aerosol for PM1 and coarse mode at the high alpine site Jungfrauoch, *Atmos. Chem. Phys.*, 8, 407–423, doi:10.5194/acp-8-407-2008, 2008b. 23711, 23725
- DeMott, P., Chen, Y., Kreidenweis, S., Rogers, D., and Sherman, D.: Ice formation by black carbon particles, *Geophys. Res. Lett.*, 26, 2429–2432, doi:10.1029/1999GL900580, 1999. 23707
- DeMott, P., Cziczo, D., Prenni, A., Murphy, D., Kreidenweis, S., Thomson, D., Borys, R., and Rogers, D.: Measurements of the concentration and composition of nuclei for cirrus formation, *P. Natl. Acad. Sci. USA*, 100, 14655–14660, 2003a. 23719
- DeMott, P., Sassen, K., Poellot, M., Baumgardner, D., Rogers, D., Brooks, S., Prenni, A., and Kreidenweis, S.: African dust aerosols as atmospheric ice nuclei, *Geophys. Res. Lett.*, 30, 1732, doi:10.1029/2003GL017410, 2003b. 23707, 23716
- Dymarska, M., Murray, B., Sun, L., Eastwood, M., Knopf, D., and Bertram, A.: Deposition ice nucleation on soot at temperatures relevant for the lower troposphere, *J. Geophys. Res.-Atmos.*, 111, D04204, doi:10.1029/2005JD006627, 2006. 23707
- Forster, P., Ramaswamy, V., Artaxo, P., Berntsen, T., Betts, R., Fahey, D., Haywood, J., Lean, J., Lowe, D., Myhre, G., et al.: Changes in atmospheric constituents and in radiative forcing, *Climate Change, The Physical Science Basis, Contribution of Working Group I to the Fourth Assessment Report of the Intergovernmental Panel on Climate Change*, edited by: Solomon,

## Ice nuclei properties at the Jungfrauoch within a Saharan Dust Event

C. Chou et al.

[Title Page](#)
[Abstract](#)
[Introduction](#)
[Conclusions](#)
[References](#)
[Tables](#)
[Figures](#)




[Back](#)
[Close](#)
[Full Screen / Esc](#)
[Printer-friendly Version](#)
[Interactive Discussion](#)


S., Qin, D., Manning, M., Chen, Z., Marquis, M., Averyt, K. B., Tignor, M., and Miller, H. L., 129–234, Cambridge Univ. Press, New York, 20, 2007. 23706

Haywood, J. and Boucher, O.: Estimates of the direct and indirect radiative forcing due to tropospheric aerosols: a review, *Rev. Geophys*, 38, 513–543, 2000. 23706

Isono, K., Komabayasi, M., and Ono, A.: The nature and origin of ice nuclei in the atmosphere, *J. Meteor. Soc. Japan*, 37, 211–233, 1959. 23707

Kamphus, M., Ettner-Mahl, M., Klimach, T., Drewnick, F., Keller, L., Cziczco, D. J., Mertes, S., Borrmann, S., and Curtius, J.: Chemical composition of ambient aerosol, ice residues and cloud droplet residues in mixed-phase clouds: single particle analysis during the Cloud and Aerosol Characterization Experiment (CLACE 6), *Atmos. Chem. Phys.*, 10, 8077–8095, doi:10.5194/acp-10-8077-2010, 2010. 23708, 23718, 23719

Kanji, Z. and Abbatt, J.: Laboratory studies of ice formation via deposition mode nucleation onto mineral dust and n-hexane soot samples, *J. Geophys. Res.-Atmos.*, 111, D16204, doi:10.1029/2005JD006766, 2006. 23712

Kanji, Z. and Abbatt, J.: Ice nucleation onto Arizona test dust at cirrus temperatures: effect of temperature and aerosol size on onset relative humidity, *J. Phys. Chem.*, 114(2), 935–941, doi:10.1021/jp908661m, 2009. 23718

Klein, H., Nickovic, S., Haunold, W., Bundke, U., Nillius, B., Ebert, M., Weinbruch, S., Schuetz, L., Levin, Z., Barrie, L. A., and Bingemer, H.: Saharan dust and ice nuclei over Central Europe, *Atmos. Chem. Phys. Discuss.*, 10, 14993–15022, doi:10.5194/acpd-10-14993-2010, 2010. 23707, 23715, 23716

Koop, T., Luo, B., Tsias, A., and Peter, T.: Water activity as the determinant for homogeneous ice nucleation in aqueous solutions, *Nature*, 406, 611–614, 2000. 23712

Lau, K. and Wu, H.: Warm rain processes over tropical oceans and climate implications, *Geophys. Res. Lett.*, 30, 2290, doi:10.1029/2003GL018567, 2003. 23707

Lohmann, U. and Feichter, J.: Global indirect aerosol effects: a review, *Atmos. Chem. Phys.*, 5, 715–737, doi:10.5194/acp-5-715-2005, 2005. 23707

Lüönd, F., Stetzer, O., Welti, A., and Lohmann, U.: Experimental study on the ice nucleation ability of size selected kaolinite particles in the immersion mode, *J. Geophys. Res.*, 115, D14201, doi:10.1029/2009JD012959, 2010. 23720

Mangold, A., Wagner, R., Saathoff, H., Schurath, U., Giesemann, C., Ebert, V., Kramer, M., and Mohler, O.: Experimental investigation of ice nucleation by different types of aerosols in the aerosol chamber AIDA: implications to microphysics of cirrus clouds, *Meteorol. Z.*, 14,

## Ice nuclei properties at the Jungfraujoch within a Saharan Dust Event

C. Chou et al.

[Title Page](#)
[Abstract](#)
[Introduction](#)
[Conclusions](#)
[References](#)
[Tables](#)
[Figures](#)




[Back](#)
[Close](#)
[Full Screen / Esc](#)
[Printer-friendly Version](#)
[Interactive Discussion](#)

485–497, 2005. 23707

Mason, B. and Maybank, J.: Ice-nucleating properties of some natural mineral dusts, *Q. J. Roy. Meteor. Soc.*, 84, 235–241, 1958. 23707

Mertes, S., Verheggen, B., Walter, S., Connolly, P., Ebert, M., Schneider, J., Bower, K., Cozic, J., Weinbruch, S., Baltensperger, U., et al.: Counterflow virtual impactor based collection of small ice particles in mixed-phase clouds for the physico-chemical characterization of tropospheric ice nuclei: sampler description and first case study, *Aerosol Sci. Tech.*, 41, 848–864, 2007. 23708, 23715, 23718

Möhler, O., Field, P. R., Connolly, P., Benz, S., Saathoff, H., Schnaiter, M., Wagner, R., Cotton, R., Krämer, M., Mangold, A., and Heymsfield, A. J.: Efficiency of the deposition mode ice nucleation on mineral dust particles, *Atmos. Chem. Phys.*, 6, 3007–3021, doi:10.5194/acp-6-3007-2006, 2006. 23707

Möhler, O., DeMott, P. J., Vali, G., and Levin, Z.: Microbiology and atmospheric processes: the role of biological particles in cloud physics, *Biogeosciences*, 4, 1059–1071, doi:10.5194/bg-4-1059-2007, 2007. 23708

Möhler, O., Georgakopoulos, D. G., Morris, C. E., Benz, S., Ebert, V., Hunsmann, S., Saathoff, H., Schnaiter, M., and Wagner, R.: Heterogeneous ice nucleation activity of bacteria: new laboratory experiments at simulated cloud conditions, *Biogeosciences*, 5, 1425–1435, doi:10.5194/bg-5-1425-2008, 2008. 23707

Nickovic, S., Kallos, G., Papadopoulos, A., and Kakaliagou, O.: A model for prediction of desert dust cycle in the atmosphere, *J. Geophys. Res.*, 106(D16), 18113–18129, doi:10.1029/2000JD900794, 2001. 23714

Nyeki, S., Li, F., Weingartner, E., Streit, N., Colbeck, I., Gäggeler, H., and Baltensperger, U.: The background aerosol size distribution in the free troposphere: an analysis of the annual cycle at a high-alpine site, *J. Geophys. Res.*, 103, 31749–31761, doi:10.1029/1998JD200029, 1998. 23717

Pérez, C., Nickovic, S., Baldasano, J., Sicard, M., Rocadenbosch, F., and Cachorro, V.: A long Saharan Dust Event over the Western Mediterranean: Lidar, sun photometer observations, and regional dust modeling, *J. Geophys. Res.*, 111, D15214, doi:10.1029/2005JD006579, 2006a. 23714

Pérez, C., Nickovic, S., Pejanovic, G., Baldasano, J., and Özsoy, E.: Interactive dust-radiation modeling: a step to improve weather forecasts, *J. Geophys. Res.*, 111, D16206, doi:10.1029/2005JD006717, 2006b. 23714

**Ice nuclei properties  
at the Jungfrauoch  
within a Saharan  
Dust Event**

C. Chou et al.

[Title Page](#)[Abstract](#)[Introduction](#)[Conclusions](#)[References](#)[Tables](#)[Figures](#)[⏪](#)[⏩](#)[◀](#)[▶](#)[Back](#)[Close](#)[Full Screen / Esc](#)[Printer-friendly Version](#)[Interactive Discussion](#)

- Petzold, A. and Schönlinner, M.: Multi-angle absorption photometry – a new method for the measurement of aerosol light absorption and atmospheric black carbon, *J. Aerosol Sci.*, 35, 421–441, 2004. 23713
- Pratt, K., DeMott, P., French, J., Wang, Z., Westphal, D., Heymsfield, A., Twohy, C., Prenni, A., and Prather, K.: In situ detection of biological particles in cloud ice-crystals, *Nat. Geosci.*, 2, 398–401, 2009. 23707
- Richardson, M., DeMott, P., Kreidenweis, S., Cziczko, D., Dunlea, E., Jimenez, J., Thomson, D., Ashbaugh, L., Borys, R., Westphal, D., et al.: Measurements of heterogeneous ice nuclei in the Western United States in springtime and their relation to aerosol characteristics, *J. Geophys. Res.*, 112, D02209, doi:10.1029/2006JD007500, 2007. 23707, 23715
- Roberts, P. and Hallett, J.: A laboratory study of the ice nucleating properties of some mineral particulates, *Q. J. Roy. Meteor. Soc.*, 94, 25–34, 1968. 23707
- Rogers, D.: Development of a continuous flow thermal gradient diffusion chamber for ice nucleation studies, *Atmos. Res.*, 22, 149–181, 1988. 23709
- Schaller, R. and Fukuta, N.: Ice nucleation by aerosol particles: experimental studies using a wedge-shaped ice thermal diffusion chamber, *J. Atmos. Sci.*, 36, 1788–1802, 1979. 23707
- Schwikowski, M., Seibert, P., Baltensperger, U., and Gaggeler, H.: A study of an outstanding Saharan Dust Event at the high-alpine site Jungfrauoch, Switzerland, *Atmos. Environ.*, 29, 1829–1842, 1995. 23714, 23718
- Stetzer, O., Baschek, B., Luond, F., and Lohmann, U.: The Zurich ice nucleation chamber (ZINC) – a new instrument to investigate atmospheric ice formation, *Aerosol Sci. Tech.*, 42, 64–74, 2008. 23708, 23710
- Vali, G.: Nucleation terminology, *Bull. Am. Meteorol. Soc.*, 66, 1426–1427, 1985. 23707
- Weingartner, E., Saathoff, H., Schnaiter, M., Streit, N., Bitnar, B., and Baltensperger, U.: Absorption of light by soot particles: determination of the absorption coefficient by means of aethalometers, *J. Aerosol Sci.*, 34, 1445–1463, 2003. 23713
- Welti, A., Lüönd, F., Stetzer, O., and Lohmann, U.: Influence of particle size on the ice nucleating ability of mineral dusts, *Atmos. Chem. Phys.*, 9, 6705–6715, doi:10.5194/acp-9-6705-2009, 2009. 23718
- Wernli, H. and Davies, H.: A Lagrangian-based analysis of extratropical cyclones. I: the method and some applications, *Q. J. Roy. Meteor. Soc.*, 123, 467–489, 1997. 23714

**Ice nuclei properties  
at the Jungfraujoch  
within a Saharan  
Dust Event**

C. Chou et al.

[Title Page](#)[Abstract](#)[Introduction](#)[Conclusions](#)[References](#)[Tables](#)[Figures](#)[◀](#)[▶](#)[◀](#)[▶](#)[Back](#)[Close](#)[Full Screen / Esc](#)[Printer-friendly Version](#)[Interactive Discussion](#)

**Table 1.** Conversion table from optical to aerodynamic diameter following Baron and Willeke (2001) and assuming an average particle density of  $1.5 \text{ g/cm}^3$  (Cozic et al., 2008b).

| optical diameter ( $\mu\text{m}$ ) | aerodynamic diameter ( $\mu\text{m}$ ) |
|------------------------------------|--|
| 0.3                                | 0.367                                  |
| 0.4                                | 0.49                                   |
| 0.5                                | 0.612                                  |
| 0.65                               | 0.796                                  |
| 0.8                                | 0.98                                   |
| 1.0                                | 1.225                                  |

## Ice nuclei properties at the Jungfraujoch within a Saharan Dust Event

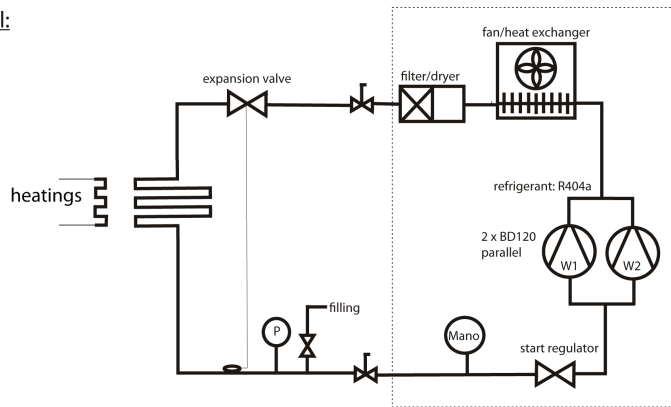
C. Chou et al.

**Table 2.** Linear regression correlation coefficient  $R^2$ , slope and offset for different cases.

| Conditions                              | $R^2$ | slope   | offset ( $\text{cm}^{-3}$ ) |
|---|-------|---------|-----------------------------|
| size class: $0.3 < D < 0.5 \mu\text{m}$ |       |         |                             |
| no dust (97 measurement points)         | 0.07  | 0.0009  | 0.0092                      |
| SDE (34 measurement points)             | 0.74  | 0.01397 | 0.06523                     |
| all days (131 measurement points)       | 0.69  | 0.01006 | -0.0231                     |
| size class: $0.5 < D < 0.8 \mu\text{m}$ |       |         |                             |
| no dust                                 | 0.13  | 0.01945 | 0.00634                     |
| SDE                                     | 0.81  | 0.04978 | 0.00586                     |
| all days                                | 0.88  | 0.05132 | -0.00259                    |

[Title Page](#)
[Abstract](#)
[Introduction](#)
[Conclusions](#)
[References](#)
[Tables](#)
[Figures](#)
[⏪](#)
[⏩](#)
[◀](#)
[▶](#)
[Back](#)
[Close](#)
[Full Screen / Esc](#)
[Printer-friendly Version](#)
[Interactive Discussion](#)

warm wall:



cold wall:

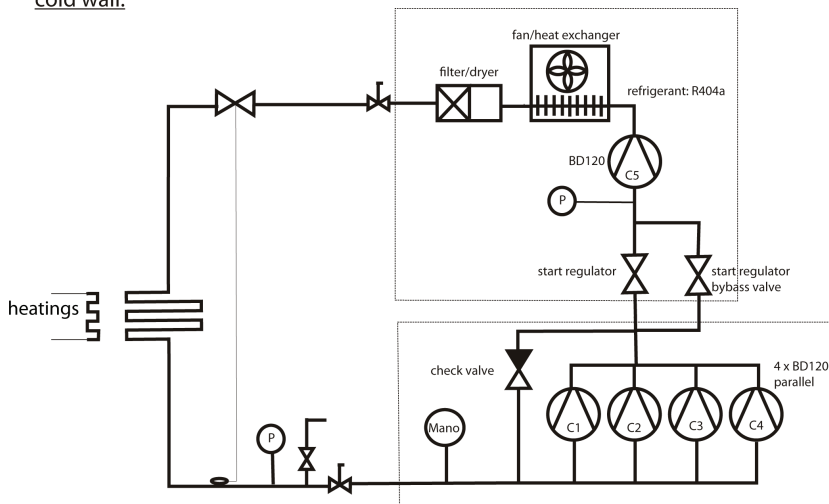


Fig. 1. Schematic of the cooling system in PINC.

23727

Title Page

Abstract

Introduction

Conclusions

References

Tables

Figures

◀

▶

◀

▶

Back

Close

Full Screen / Esc

Printer-friendly Version

Interactive Discussion

**Ice nuclei properties at the Jungfrauoch within a Saharan Dust Event**

C. Chou et al.

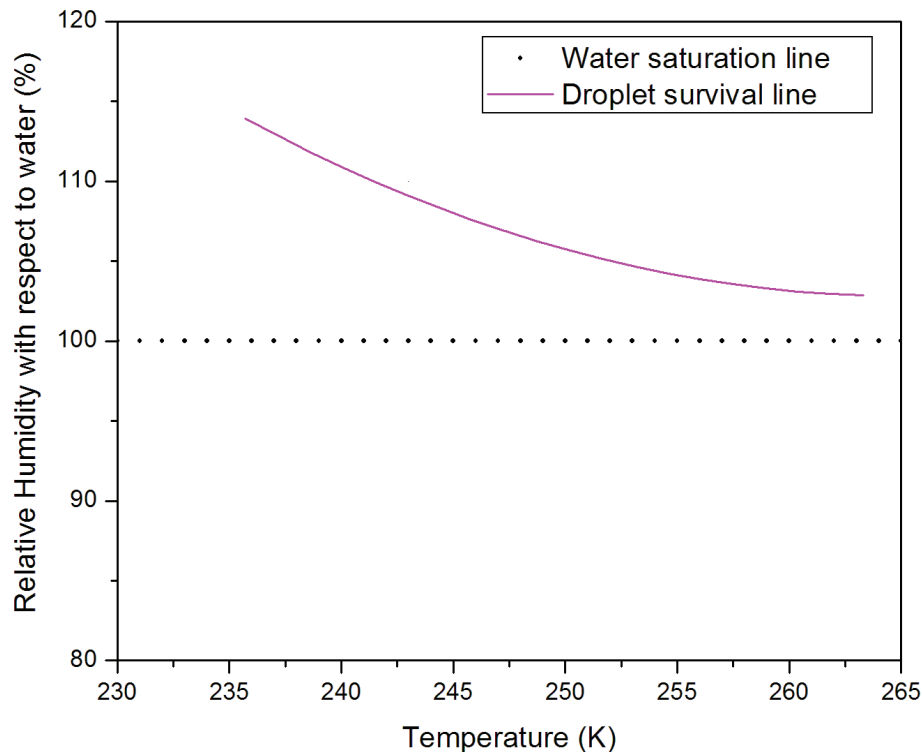


**Fig. 2.** Experimental determination of the water droplet survival line (water breakthrough) for different temperatures. Above the droplet survival line, the OPC can not distinguish ice crystals and water droplets.

[Title Page](#)[Abstract](#)[Introduction](#)[Conclusions](#)[References](#)[Tables](#)[Figures](#)[◀](#)[▶](#)[◀](#)[▶](#)[Back](#)[Close](#)[Full Screen / Esc](#)[Printer-friendly Version](#)[Interactive Discussion](#)

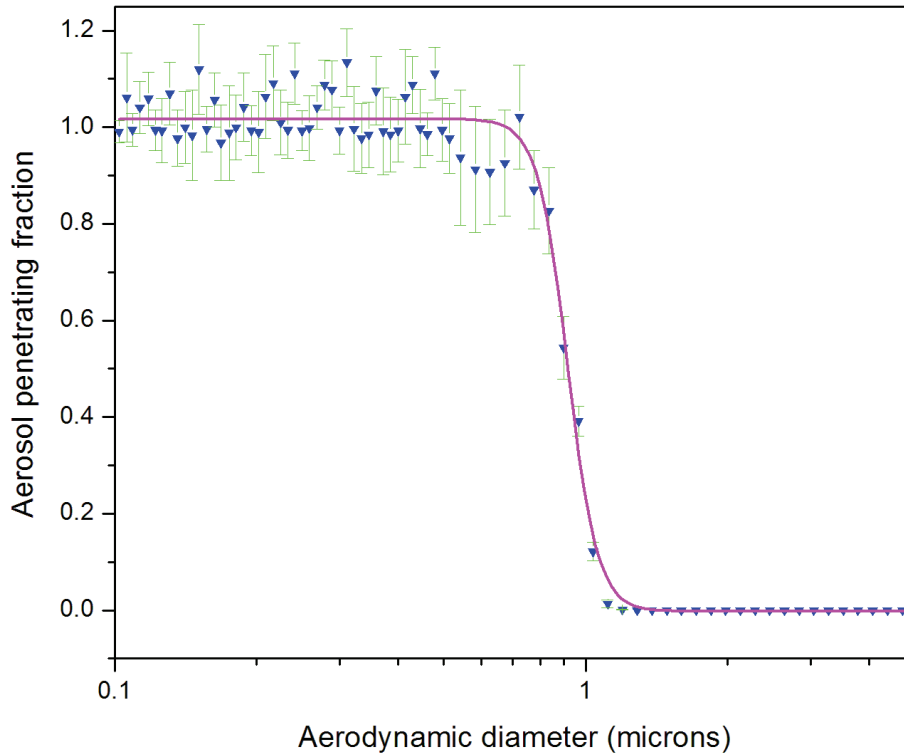


**Fig. 3.** Aerosol penetrating fraction of the impactor used. Note the sharp cut-off at  $1\ \mu\text{m}$  aerodynamic diameter. The magenta curve is the sigmoid fit of the blue data points. Green error bars represent the standard deviation of the measurements.

**Ice nuclei properties at the Jungfraujoch within a Saharan Dust Event**

C. Chou et al.

|                          |              |
|--------------------------|--------------|
| Title Page               |              |
| Abstract                 | Introduction |
| Conclusions              | References   |
| Tables                   | Figures      |
| ◀                        | ▶            |
| ◀                        | ▶            |
| Back                     | Close        |
| Full Screen / Esc        |              |
| Printer-friendly Version |              |
| Interactive Discussion   |              |



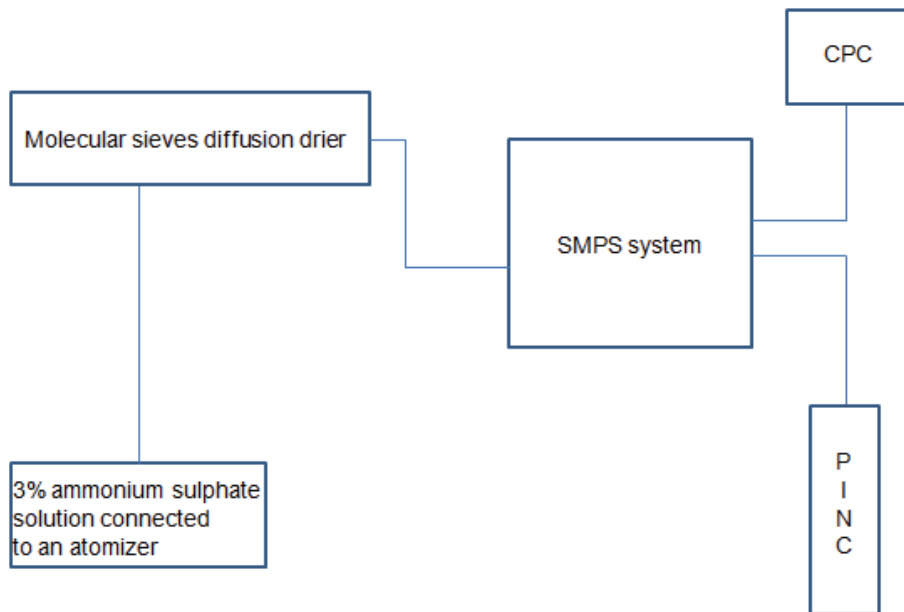


**Fig. 4.** Experimental setup to study the deliquescence point of ammonium sulphate at  $-30^{\circ}\text{C}$  and freezing of AS at  $-40^{\circ}\text{C}$ .

**Ice nuclei properties at the Jungfraujoch within a Saharan Dust Event**

C. Chou et al.

|                          |              |
|--------------------------|--------------|
| Title Page               |              |
| Abstract                 | Introduction |
| Conclusions              | References   |
| Tables                   | Figures      |
| ⏪                        | ⏩            |
| ◀                        | ▶            |
| Back                     | Close        |
| Full Screen / Esc        |              |
| Printer-friendly Version |              |
| Interactive Discussion   |              |



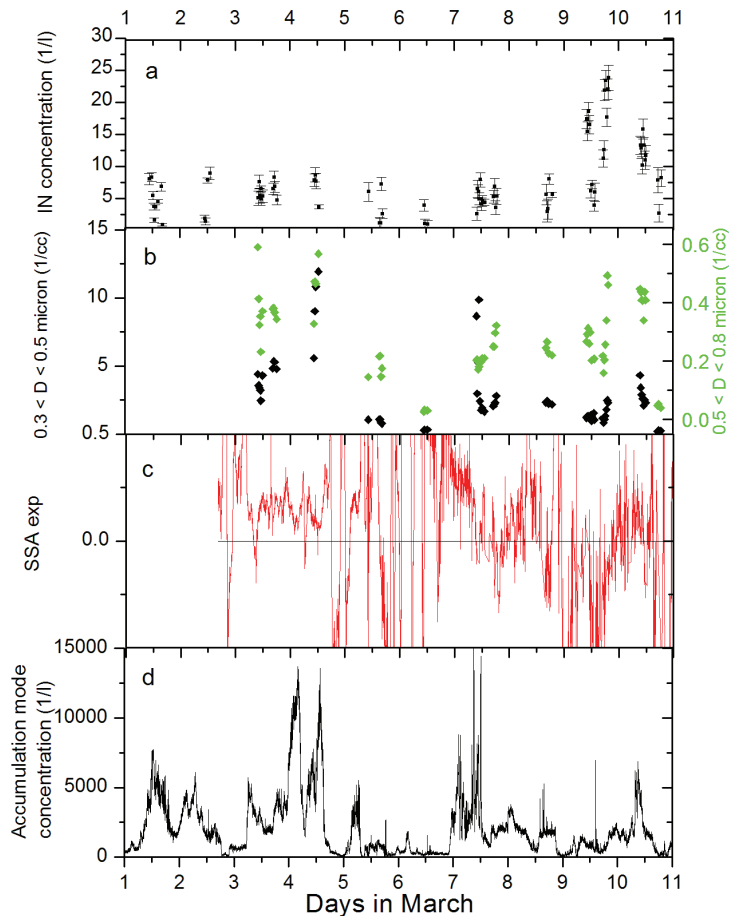


**Fig. 5.** (a) Time series of the 15 min IN average number concentration (particles/liter) from 1 to 11 March 2009. (b) Particles concentration per size class. (c) Single Scattering Albedo (SSA) exponent value. (d) Particles number concentration in the accumulation mode.

## Ice nuclei properties at the Jungfraujoch within a Saharan Dust Event

C. Chou et al.

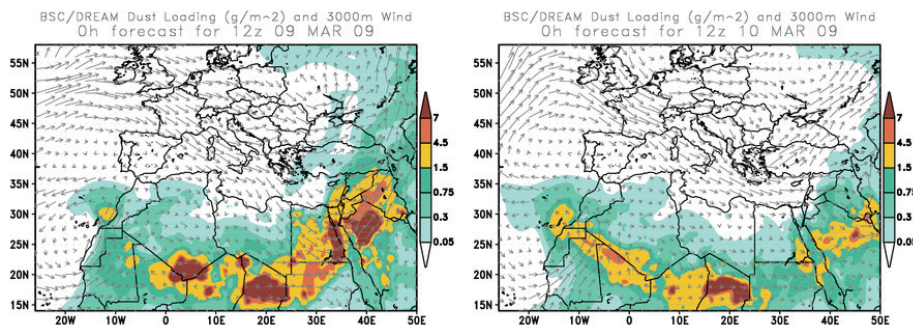


**Fig. 6.** Dust load distribution over the Mediterranean region on 9 and 10 March 2009 at 12:00 p.m. UTC.

[Title Page](#)[Abstract](#)[Introduction](#)[Conclusions](#)[References](#)[Tables](#)[Figures](#)[◀](#)[▶](#)[◀](#)[▶](#)[Back](#)[Close](#)[Full Screen / Esc](#)[Printer-friendly Version](#)[Interactive Discussion](#)



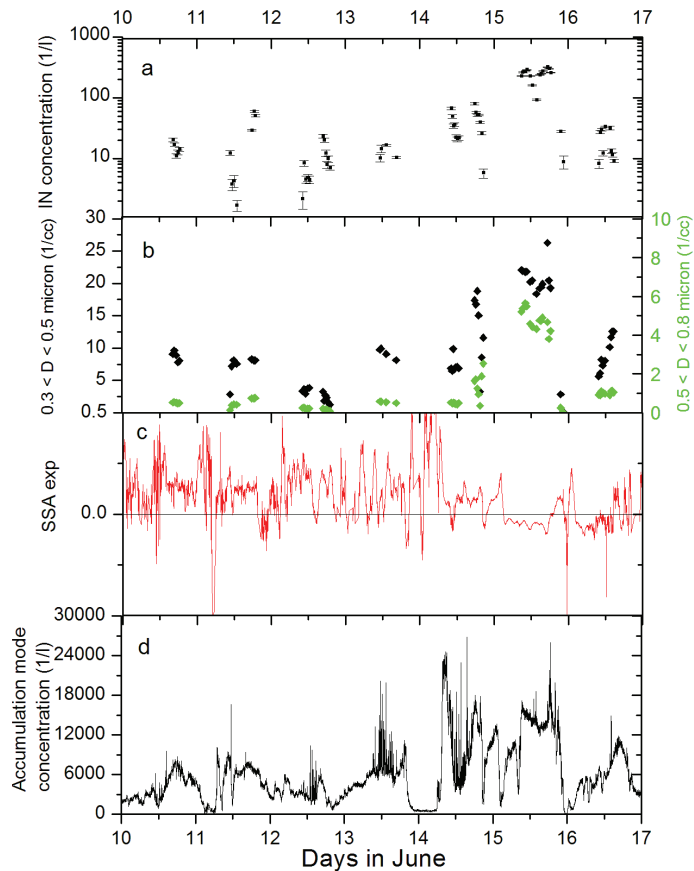


**Fig. 8.** (a) Time series of IN average number concentration (particles/liter) from 10 to 16 June 2009. (b) Particles concentration per size class. (c) Single Scattering Albedo (SSA) exponent value. (d) Particles number concentration in the accumulation mode.

## Ice nuclei properties at the Jungfraujoch within a Saharan Dust Event

C. Chou et al.

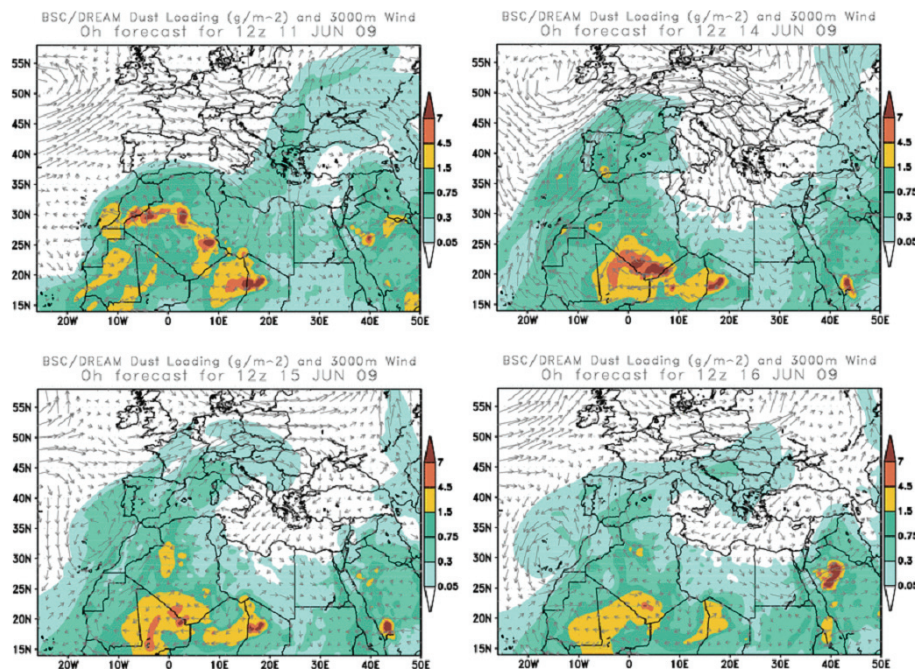


**Fig. 9.** Dust load distribution over the Mediterranean region on 11, 14, 15 and 16 June 2009 at 12:00 p.m. UTC.

[Title Page](#)[Abstract](#)[Introduction](#)[Conclusions](#)[References](#)[Tables](#)[Figures](#)[◀](#)[▶](#)[◀](#)[▶](#)[Back](#)[Close](#)[Full Screen / Esc](#)[Printer-friendly Version](#)[Interactive Discussion](#)

## Ice nuclei properties at the Jungfraujoch within a Saharan Dust Event

C. Chou et al.

Title Page

Abstract

Introduction

Conclusions

References

Tables

Figures

◀

▶

◀

▶

Back

Close

Full Screen / Esc

Printer-friendly Version

Interactive Discussion

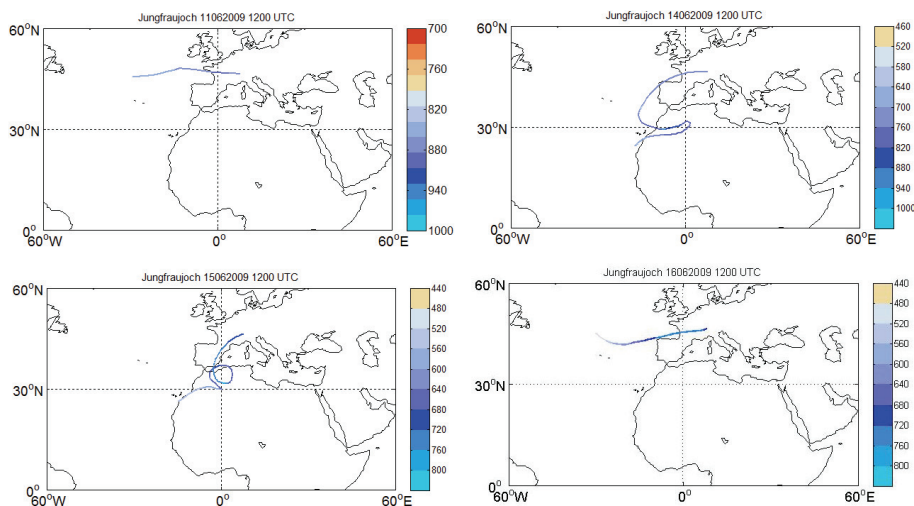


**Fig. 10.** Four days backtrajectories on 11, 14, 15 and 16 June 2009 at Jungfraujoch at 12:00 p.m. UTC.

## Ice nuclei properties at the Jungfraujoch within a Saharan Dust Event

C. Chou et al.

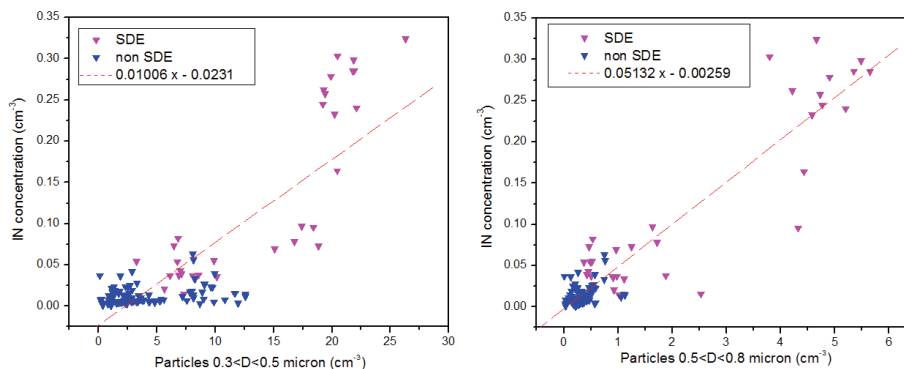


**Fig. 11.** IN number concentration versus particles number concentration of different size classes: blue triangles represents non SDE measurements and magenta ones, SDE measurements.

[Title Page](#)[Abstract](#)[Introduction](#)[Conclusions](#)[References](#)[Tables](#)[Figures](#)[⏪](#)[⏩](#)[◀](#)[▶](#)[Back](#)[Close](#)[Full Screen / Esc](#)[Printer-friendly Version](#)[Interactive Discussion](#)

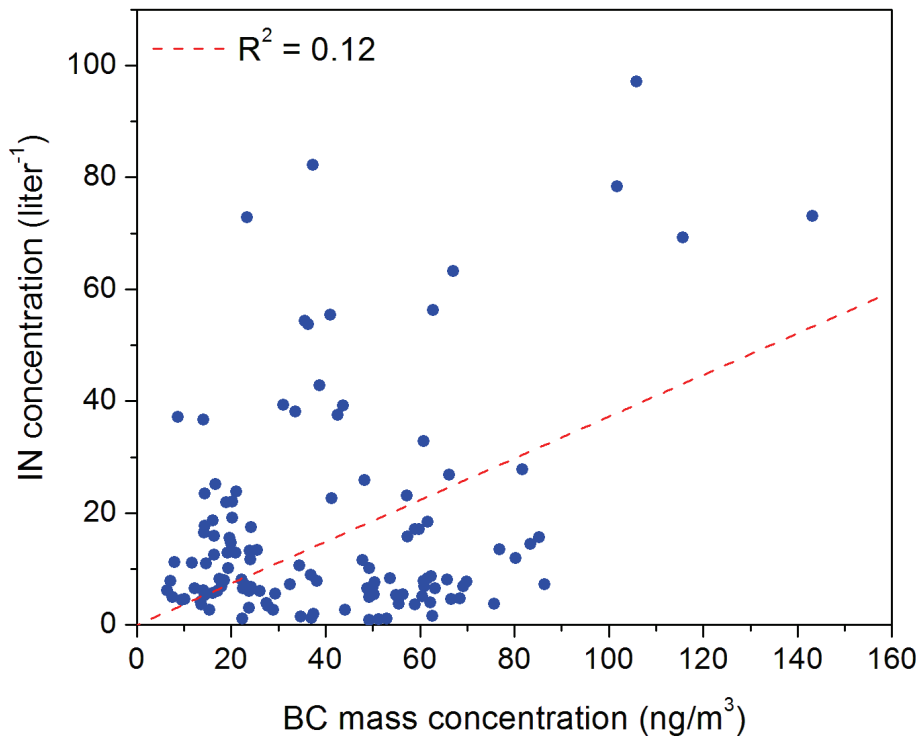


**Fig. 12.** IN number concentration versus BC concentration during PINC II and III on clear days.

**Ice nuclei properties at the Jungfrauoch within a Saharan Dust Event**

C. Chou et al.

|                          |              |
|--------------------------|--------------|
| Title Page               |              |
| Abstract                 | Introduction |
| Conclusions              | References   |
| Tables                   | Figures      |
| ◀                        | ▶            |
| ◀                        | ▶            |
| Back                     | Close        |
| Full Screen / Esc        |              |
| Printer-friendly Version |              |
| Interactive Discussion   |              |

